Simultaneous seismic reflection and physical oceanographic observations of oceanic fine structure in the Kuroshio extension front

Y. Nakamura,[1] T. Noguchi,[1] T. Tsuji,[1] S. Itoh,[1] H. Niino,[1] and T. Matsuoka[2]

Received 3 July 2006; revised 2 October 2006; accepted 18 October 2006; published 8 December 2006.

[1] New simultaneous seismic reflection and physical oceanographic observations east of Japan demonstrate the utility of the seismic reflection method in mapping oceanic fine structure. Synthetic seismograms calculated from temperature and salinity data confirm that seismic reflections correlate with physical oceanographic structures. Seismic reflections at the boundary between the warm Kuroshio and the cold Oyashio water masses correspond to well developed, ~10 m scale, temperature fine structure. Vertical current profiles suggest that this fine structure is caused by interleaving of these two water masses. We compare our seismic images with acoustic Doppler current profiler (ADCP) intensity maps and discuss similarities and the differences between seismic images and the ADCP maps. Our study demonstrates that even relatively low-energy seismic sources, in this case a 3.4 l (210 in^3) generator-injector (GI) airgun, can be used to image upper oceanic fine structure. **Citation:** Nakamura, Y., T. Noguchi, T. Tsuji, S. Itoh, H. Niino, and T. Matsuoka (2006), Simultaneous seismic reflection and physical oceanographic observations of oceanic fine structure in the Kuroshio extension front, *Geophys. Res. Lett.*, *33*, L23605, doi:10.1029/2006GL027437.

1. Introduction

[2] Oceanic fine structure commonly develops at boundaries between different water masses. Understanding fine structure is critical to studies of large-scale thermohaline circulation, which is widely recognized to play a crucial role in global climate change and therefore the Earth system [e.g., *Thorpe*, 2005]. Physical oceanographers typically investigate fine structure using vertical profiles of temperature and salinity [e.g., *Moum*, 1998]. Because most physical oceanographic measurements are made at discrete locations, the horizontal scale and continuity of fine structure are not well understood. Therefore, 2D and 3D mapping of fine structure is of great interest to the physical oceanographic community and beyond [e.g., *Stommel and Fedorov*, 1967].

[3] Recently *Holbrook et al.* [2003] demonstrated that the seismic reflection method can image thermohaline fine structure as reflection events within the water column, following previous pioneering studies on such events in seismic data [*Gonella and Michon*, 1988; *Phillips and Dean*, 1991]. *Nandi et al.* [2004] conducted the first simultaneous seismic reflection and physical oceanographic observations, in the Norwegian Sea, to confirm the utility of the seismic reflection method in studying oceanic fine structure, and showed that the method has a temperature sensitivity of ~0.03°C. In the same region, *Holbrook and Fer* [2005] analyzed seismic reflections to reveal oceanic internal wave spectra, and *Páramo and Holbrook* [2005] undertook amplitude versus offset (AVO) analysis to quantify temperature contrasts remotely from seismic reflection data. South of Japan, *Tsuji et al.* [2005] imaged fine structure related to the Kuroshio current, using data from a 3D seismic volume. They showed that coherent fine structure can persist for at least 20 days. Overall, multidisciplinary "Seismic Oceanography" [*Holbrook et al.*, 2005] should greatly advance our understanding of oceanic fine structure.

[4] Herein, we report results of simultaneous seismic reflection and physical oceanographic (temperature, salinity, and current speed profile) investigations conducted in the boreal summer of 2005. Our survey area encompassed the Kuroshio extension front east of Japan (Figure 1a), where the warm Kuroshio current flowing generally northeastward meets cold Oyashio water. The front is the boundary between the two water masses characterized by different temperature and salinity profiles. At the front, the two water masses mix, and fine structure is likely to be well developed (Figure 1b) in the vicinity. We analyze the new seismic reflection data for fine structure, and use simultaneous oceanographic measurements for "ground truth."

2. Data and Analysis

[5] All data used in this study were obtained during the 2005 R/V *Tansei Maru* cruise KT05-21, the first-ever expedition devoted exclusively to joint seismic reflection and physical oceanographic observations for the purpose of studying oceanic fine structure. Within the Kuroshio extension front area east of Japan (Figure 1a), our two-line transect runs N-S, or perpendicular to the axis of the Kuroshio current. The surface current is too fast (~3.5–4kt) at the Kuroshio's axis to conduct a seismic reflection survey, so we acquired two separate survey lines, one north (Line 1: 111 km long) and one south (Line 2: 83 km long) of the main Kuroshio current axis.

[6] We acquired multi-channel seismic (MCS) data using a 48-channel, 1200 m streamer. The data were recorded at a 2 ms sampling interval. We employed three different single airgun configurations as seismic sources: a 20 l (1220 inch^3) airgun, a 9 l (550 inch^3) airgun, and a 3.4 l (210 inch^3) generator-injector (GI) airgun. We shot Line 1 three times, once each with the three different seismic sources. At R/V *Tansei Maru*'s shooting speed of ~7.5 km/hr, shot intervals of 75 s for the 20 l airgun, 40 or 50 s for the 9 l airgun, and

[1]Ocean Research Institute, University of Tokyo, Tokyo, Japan.
[2]Graduate School of Engineering, Kyoto University, Kyoto, Japan.

0094-8276/06/2006GL027437

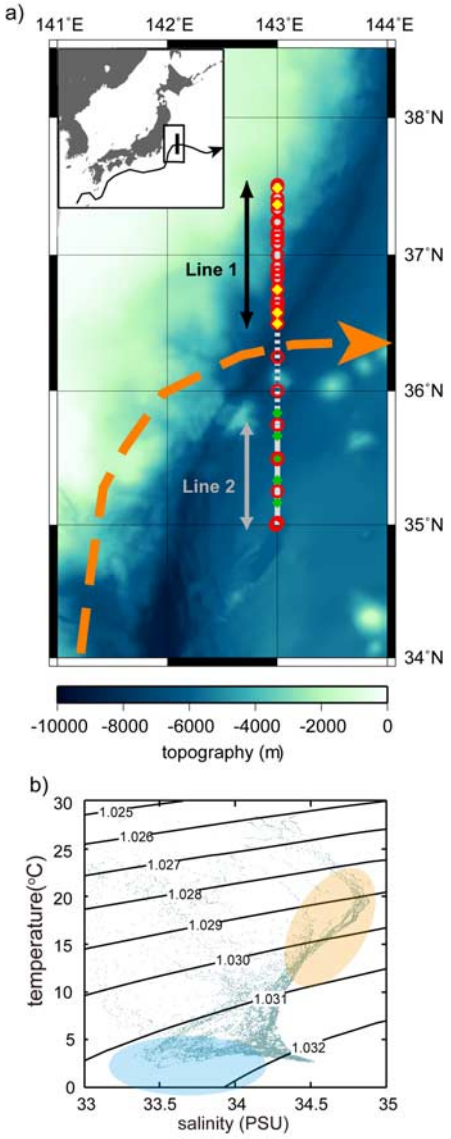

Figure 1. (a) Bathymetric map of the study area. Thick gray lines running along 143°E indicate the two seismic reflection lines, the extents of which are indicated by arrows. Expendable conductivity-temperature-depth (XCTD), expendable bathythermograph (XBT), and expendable current profiler (XCP) casts are indicated by red open circles, green diamonds, and yellow diamonds, respectively. The Kuroshio extension front is depicted by an orange dashed line. Inset shows regional context of the R/V *Tansei Maru* KT05-21 (28 August–3 September 2005) survey area (rectangle), the location of the seismic reflection/physical oceanographic transect (thick black line), and the location of the Kuroshio current axis, extension, and flow direction (meandering black line with arrow). (b) Temperature-salinity plot from expendable conductivity-temperature-depth (XCTD) measurements. PSU means "Practical Salinity Unit." Dots in the orange oval correspond to higher temperature water associated with the Kuroshio current, and those in the blue oval to lower temperature water associated with the Oyashio current. Isopycnal curves are depicted by black thin lines; densities are in kg/m^3. All data plotted here were obtained by the XCTD casts shown in Figure 1a between 29 August and 1 September 2005.

20 s for the 3.4 l airgun corresponded to approximately 150, 80–100, and 40 m, respectively. The GI gun was fired in "harmonic mode", which generates a broader, but larger signal compared with shooting in true GI mode. The towing depth of the airgun was 5–7 m for the 9 l and 20 l airguns, and 3 m for the 3.4 l airgun. The streamer cable was towed at 7 m depth. Expendable bathythermograph (XBT), expendable conductivity-temperature-depth (XCTD) and expendable current profiler (XCP) measurements were also conducted to obtain vertical profiles of water properties during acquisition of the MCS data. Thirteen XCTDs and 4 XCPs were deployed along the 20 l airgun line, 1 XCTD along the 9 l airgun line, and 9 XCTDs and 1 XCP along the 3.4 l airgun line. South of Kuroshio front, we shot Line 2 with the 9 l airgun, and conducted 4 XBT and 2 XCTDs casts. Before starting MCS data acquisition, we deployed 11 XCTDs to obtain an overview of the thermohaline structure in the study area.

[7] The MCS data were processed conventionally with geometry definition, deconvolution, common mid-point (CMP) sorting, normal moveout (NMO), stacking, and 12–100 Hz bandpass filtering [*Yilmaz*, 2001]. Two-dimensional dip filtering and a near-trace mute were also applied to suppress direct wave and bubble pulse energy. Commercial softwares were used to process the MCS data. We adopted a velocity model derived from XCTD measurements for the normal moveout correction, and the stacked sections were converted to depth sections using the same velocity. We employed the depth sections to examine fine structure within the water column together with vertical profiling data from XBT, XCTD and XCP casts. Acoustic Doppler current profiler (ADCP) data were also acquired throughout the entire survey.

3. Results and Discussions

[8] Seismic reflection events in the study area correlate with temperature and salinity changes in the water column at depths of 200–800 m (Figure 2). North of Kuroshio extension front (Line 1; Figures 1a and 2b–2d), reflection events are similar on sections acquired with the three different seismic sources. On the northern part of Line 1, the apparent dip of the reflections is shallow to the south at depths of ~200 m. On the southern part of Line 1, the apparent dip of the reflections is steeper down to ~500 m depths. XCTD data obtained simultaneously with the MCS data reveal the physical and chemical cause of the reflections. We calculated synthetic reflection seismograms using salinity and temperature data [*Tsuji et al.*, 2005]. The center frequency of the Ricker wavelet used to calculate synthetic seismograms was 30 Hz for the 9 l and 20 l airgun lines, and 40 Hz for the 3.4 l airgun line. The synthetics match quite well with the MCS data. Large amplitude events and their depths correlate well between the two, indicating that the reflections in the MCS sections reflect true oceanic structure in the water column. South of Kuroshio extension front (Line 2; Figures 1 and 2e), reflections are present at depths of 700–800 m. On the northern part of Line 2, reflections are discontinuous, with a slight apparent dip to the south, whereas on the southern part, they are sub-parallel to the sea surface at depths of ~800 m. Along Line 2, operational challenges, such as the disconnection of probe wire prob-

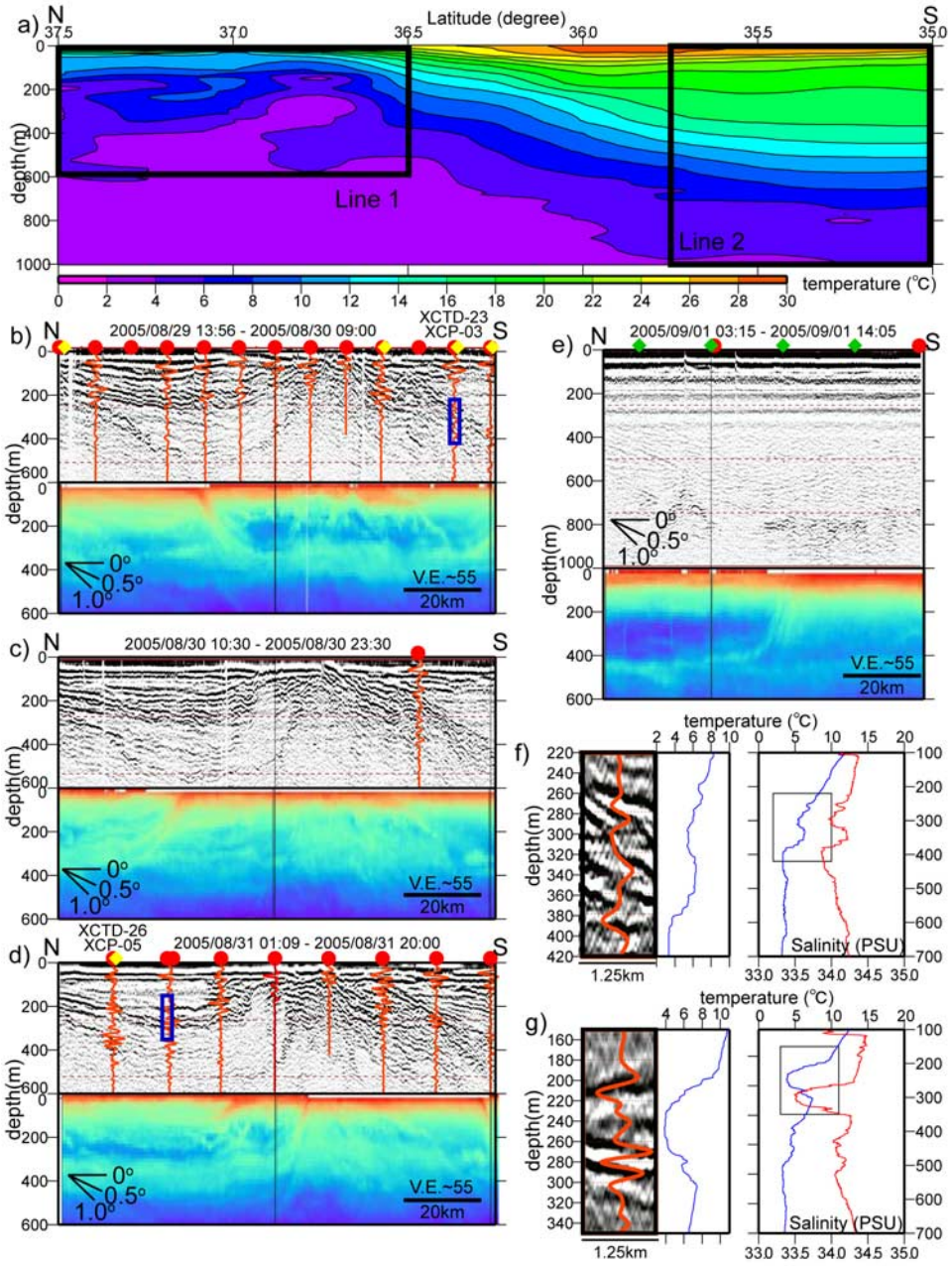

Figure 2. Major results of this study (see Figure 1a for location). (a) Temperature profile derived from expendable conductivity-temperature-depth (XCTD) measurements. (b) Seismic reflection profile (top) and acoustic Doppler current profile (ADCP) intensity (bottom) for Line 1 using a 20 l airgun. Time period of observation is indicated above the seismic profile. Red circles, green diamonds, and yellow diamonds are XCTD, expendable bathythermograph (XBT), and expendable current profiler (XCP) locations, respectively. Red waveforms on the seismic reflection profiles are synthetic seismograms calculated from XCTD data. For expanded data in blue rectangle, see Figure 2f, left middle. (c) Same as Figure 2b except using a 9 l airgun. (d) Same as Figure 2b except using a 3.4 l airgun. For expanded data in blue rectangle, see Figure 2g, left middle. (e) Same as Figure 2b except data are from Line 2, and the seismic reflection profile extends to a depth of 1000 m. (f) Comparison of Line 1 seismic reflection profile (20 l airgun) and XCTD data. Seismic profile overlain by a synthetic seismogram (red line) (left). Temperature (blue) and salinity (red) profiles derived from XCTD measurements (right). Blow-up of temperature data from the black rectangle to the right, which corresponds to the depth range of the seismic reflection profile to the left (middle). See Figure 2b for location (blue rectangle). (g) Same as Figure 2f except using 3.4 l airgun. See Figure 2d for location (blue rectangle).

ably due to entanglement with the streamer cable or the towing harness of the airgun, prevented simultaneous acquisition of XCTD/XBT and MCS data where the reflections were present. Nevertheless, we were able to document fine structure via XCTD measurements conducted approximately three days before MCS data acquisition, and the depths of the fine structure generally match the depths of reflection events.

[9] Seismic reflections also correlate with changes in ADCP scattering intensity profiles (Figures 2b–2e). Along Line 1, general features, including the apparent dips of structure and geographic locations, are similar for MCS and ADCP data, although ADCP intensity pattern appears to have a more complicated distribution than reflections in the MCS profiles. For example, ADCP maps show more steeply dipping patterns (e.g., ~30 km south of the northern end of Line 1 in Figure 2b), but such patterns are not clear in the seismic profiles. In contrast, along Line 2, ADCP data show significant intensity changes at approximately 400 m depth, but the only prominent seismic reflections lie deeper at 700–800 m. Differences between ADCP intensity maps and MCS profiles might arise from different frequency contents of the sound sources, 78 kHz and <100 Hz, respectively, which result in differing spatial resolutions, signal attenuations (penetration depths), and sensitivities to fine structure. With respect to the latter, the ADCP method is sensitive to scattering phenomena such as plankton blooms, whereas MCS reflections mark changes in acoustic impedance, which is the product of density and acoustic velocity. ADCP intensity maps may not directly represent thermohaline structure, but rather density differences of plankton and suspended material in different water masses.

[10] Fine structure in XCTD observations of temperature and salinity (Figures 2f and 2g) occurs on a vertical scale of approximately 10 m where seismic reflections were imaged. This fine structure scale is comparable to that observed in the Norwegian Sea [*Nandi et al.*, 2004], and smaller than that observed in the Kuroshio Current [*Tsuji et al.*, 2005]. In our study, the dominant frequencies of seismic sources were ~25 Hz for the 20 l and 9 l airguns, and ~35 Hz for the 3.4 l airgun, corresponding to vertical resolutions of ~15 m and ~10 m, respectively, assuming the Rayleigh resolution limit of 1/4 wavelength. We were able to image fine structure of approximate 10 m scale seismically because the dominant vertical scale of fine structure was large enough to be resolvable by acoustic waves from the airguns.

[11] Seismically imaged structure with an apparent southward dip can be correlated with temperature profiles of the water column (Figures 2a–2e). Reflectors appear where water temperatures range between 4 and 8 °C, which is at the base of the thermocline. This observation resembles that in the Norwegian Sea [*Nandi et al.*, 2004]. Comparisons of MCS profiles, XCTD-derived temperatures, and XCP-derived current velocities (Figure 3) reveal that water moves northward above the prominent reflection at a depth of ~200 m, while it moves southward beneath. We interpret this polarity change in current velocity correlative with a seismic reflection as the boundary between the warm Kuroshio water mass and the cold Oyashio water mass. At this boundary, interleaving and mixing of Kuroshio and Oyashio water masses cause the oceanic fine structure (Figure 1b). Fine structure in the Kuroshio extension front appears to persist for at least a few days, judging from our repetitive MCS experiments along Line 1. *Tsuji et al.* [2005] reported that fine structure was observed for more than 20 days along the Kuroshio front south of Japan.

[12] Three different airguns were used for MCS data acquisition along Line 1 (Figure 2). General features of the three Line 1 MCS profiles are similar, as discussed above, but characteristics of the images differ due to

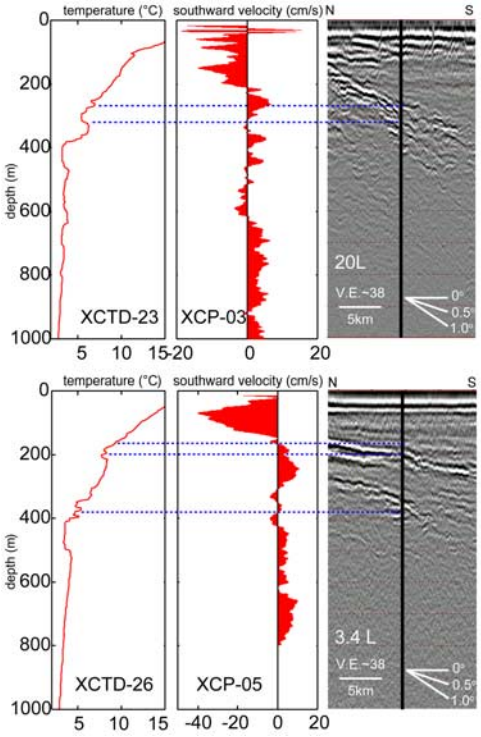

Figure 3. Comparison of (left) expendable conductivity-temperature-depth (XCTD) temperature, (middle) expendable current profiler (XCP) southward velocity, and (right) seismic reflection data. See Figures 1 and 2 for location. The current data were low-cut filtered with a corner frequency at 10 m. Thin dashed blue horizontal lines indicate abrupt temperature and velocity changes correlative with seismic reflections. Thin black vertical lines on the seismic reflection data indicate locations of the XCTD and XCP casts in Figure 3, right. (top) Data from Line 1 shot with a 20 l airgun, (bottom) data from Line 1 shot with a 3.4 l airgun. These two measurements were separated in time by ~19 hours.

variations in seismic source energy (volumes of chambers) and shapes of source signatures. For example, the 20 l airgun generated the most energy, which favored imaging fine structure characterized by small acoustic impedance contrasts, but large amplitude bubble pulses caused a low quality source signature. On the other hand, the 3.4 l airgun produced the least energy, but the large peak-to-bubble ratio characteristic of GI-type airguns is favorable for exploring oceanic fine structure, the details of which are commonly contaminated by the bubble pulses of other sources. Our choice for the low-cut frequency in bandbass filtering and the near-trace mute aimed to reduce the large amplitude bubble pulse that especially affect the 9 l and 20 l profiles; it helped to improve the quality of the profiles. MCS data quality is also affected by the signal-to-noise ratio, which is related to the fold of the CMP gathers. The shot interval for the 3.4 l airgun was the shortest, and for the 20 l the longest, yielding the largest fold (typically 16) for the data shot with the former, and the lowest fold (typically 4) for the latter. Most surprisingly, MCS data acquired with the 3.4 l airgun successfully imaged fine structure characterized by ~0.5°C temperature contrasts at depths shallower than 500 m. This

seismic source is much smaller than those used in previous studies; e.g., 22 l [*Nandi et al.*, 2004] and ~70 l [*Tsuji et al.*, 2005]. The disadvantage of the small volume of the 3.4 l airgun was compensated for by a better source signature and a larger fold. Use of GI-type airguns producing minimal bubble pulses, as well as of tuned airgun arrays producing large peak-to-bubble ratios, will be important in obtaining more detailed images of thermohaline structure.

4. Summary and Conclusions

[13] Simultaneous seismic reflection and physical oceanographic observations across the Kuroshio extension front have yielded new scientific and methodological insights. Seismic reflections between 200 and 800 m deep and apparently dipping southward were investigated and compared with in situ physical oceanographic measurements, and the reflections were confirmed to originate from oceanic fine structure. The seismic reflections were observed at the boundary between two water masses with different thermohaline characteristics, where mixing of the two causes fine structure to develop. For the first time, current profiling was conducted simultaneously with MCS data acquisition, and the data indicate that the reflections are situated at the boundary of water flowing in opposite directions, perpendicular to the axis of the front. Results from repetitive MCS surveys with different seismic sources has documented the capability of a 3.4 l airgun to map oceanic fine structure, at least in depths shallower than ~500 m, which will contribute to future research in "Seismic Oceanography."

[14] **Acknowledgments.** We are grateful to Captain F. Inaba and the entire crew of R/V *Tansei Maru* for their kind support in conducting observations during cruise KT05-21. T. Kodera and Y. Ohwatari of Nippon Marine Enterprises, Ltd., and K. Kameo of the Ocean Research Institute, University of Tokyo, are acknowledged for their technical support during the cruise. Y. Kajiwara and A. Obi of the University of Tokyo, and K. Shiraishi, M. Kato, and H. Tokunaga of Kyoto University helped with observations and preliminary onboard data processing. The authors thank M. Coffin, R. Hobbs, and an anonymous reviewer for their helpful comments and suggestions. This study was supported by Ocean Research Institute joint research funds. Some figures were made with Generic Mapping Tools software.

References

Gonella, J., and D. Michon (1988), Deep internal waves measured by seismic-reflection within the eastern Atlantic water mass (in French with English abstract), *C. R. Acad. Sci. Ser. II*, *306*, 781–787.

Holbrook, W. S., and I. Fer (2005), Ocean internal wave spectra inferred from seismic reflection transects, *Geophys. Res. Lett.*, *32*, L15604, doi:10.1029/2005GL023733.

Holbrook, W. S., P. Paramo, S. Pearse, and R. W. Schmitt (2003), Thermohaline fine structure in an oceanographic front from seismic reflection profiling, *Science*, *301*, 821–824.

Moum, J. N. (1998), Quantifying vertical fluxes from turbulence in the ocean, *Oceanography*, *10*, 111–115.

Nandi, P., W. S. Holbrook, S. Pearse, P. Páramo, and R. W. Schmitt (2004), Seismic reflection imaging of water mass boundaries in the Norwegian Sea, *Geophys. Res. Lett.*, *31*, L23311, doi:10.1029/2004GL021325.

Páramo, P., and W. S. Holbrook (2005), Temperature contrasts in the water column inferred from amplitude-versus-offset analysis of acoustic reflections, *Geophys. Res. Lett.*, *32*, L24611, doi:10.1029/2005GL024533.

Phillips, J. D., and D. F. Dean (1991), Multichannel acoustic reflection profiling of ocean watermass temperature/salinity interfaces, in *Ocean Variability and Acoustic Propagation*, edited by J. Potter and A. Warn-Varnas, pp. 199–214, Springer, New York.

Stommel, H., and K. N. Fedorov (1967), Small scale structure in temperature and salinity near Timor and Mindanao, *Tellus*, *19*, 306–325.

Thorpe, S. A. (2005), *The Turbulent Ocean*, 439 pp., Cambridge Univ. Press, New York.

Tsuji, T., T. Noguchi, H. Niino, T. Matsuoka, Y. Nakamura, H. Tokuyama, S. Kuramoto, and N. Bangs (2005), Two-dimensional mapping of fine structures in the Kuroshio Current using seismic reflection data, *Geophys. Res. Lett.*, *32*, L14609, doi:10.1029/2005GL023095.

Yilmaz, O. (2001), *Seismic Data Processing: Processing, Inversion, and Interpretation of Seismic Data*, *Invest. Geophys. Ser.*, vol. 10, 2nd ed., edited by S. M. Doherty, Soc. of Explor. Geophys., Tulsa, Okla.

S. Itoh, Y. Nakamura, H. Niino, T. Noguchi, and T. Tsuji, Ocean Research Institute, University of Tokyo, 1-15-1 Minamidai, Nakano-ku, Tokyo 164-8639, Japan. (saru@ori.u-tokyo.ac.jp)

T. Matsuoka, Graduate School of Engineering, Kyoto University, Kyoto Daigaku Katsura, Nishikyo-ku, Kyoto 615-8530, Japan.